Electronic Supporting Information (ESI):

Lanthanide anthracene complexes: slow magnetic relaxation and luminescence in Dy^{III}, Er^{III} and Yb^{III} based materials

Qian Zou, Xin-Da Huang, Jing-Cui Liu, Song-Song Bao and Li-Min Zheng*

Table S1. A list of molecular formulas and alternating magnetic properties for compounds that have been reported to contain anthracene–based ligands and lanthanide metal salts.

Compounds formula	Structure	Magnetic properties (U_{eff} /K)	Ref.
$[Dy(L^1)_2(NO_3)(DMF)_2]$	mononuclear	SMM, 23 (1 kOe)	1
$[Yb(L^1)_3(Py)]$	mononuclear	n.a.[f]	1
$\{[Nd(L^2)_{1.5}(DMF)_2]\cdot(DMF)\}_n$	3D MOF	field-SMM, 22.9 (1 kOe)	2
$\{[Dy(L^2)_{1.5}(DMF)_2]\cdot(DMF)\}_n$	3D MOF	SMM, 52.7 (1 kOe)	2
$\{[Gd(L^2)_{1.5}(DMF)_2]\cdot(DMF)\}_n$	3D MOF	field-SMM, 15.4 (1 kOe)	2
$\{[Er(L^2)_{1.5}(DMF)_2]\cdot(DMF)\}_n$	3D MOF	field-SMM, 13.0 (1 kOe)	2
$\{[Yb(L^2)_{1.5}(DMF)_2]\cdot(DMF)\}_n$	3D MOF	field-SMM, 22.9 (1 kOe)	2
$\{[Yb(L^2)(NO_3)(DMF)_2]\cdot(DMF)_{0.33}\}_n$	2D MOF	field-SMM, 16.2 (1 kOe)	2
$[Dy(hfac)_3(L^3)(H_2O)]$[a]	mononuclear	field-SMM, 13.4 (1 kOe)	3
$[Dy(hfac)_3(L^3)_2]_2\cdot H_2O$	mononuclear	field-SMM	3
$[Dy_2(\mu_2\text{-}L^4)_4(L^4)_2(bpy)_2]$	dinuclear	SMM, 51.2 (0 Oe)	4
$[Dy_2(\mu_2\text{-}L^4)_4(L^4)_2(phen)_2]$	dinuclear	SMM, 49.4 (0 Oe)	4
$[Dy_2(\mu_2\text{-}L^4)_4(L^4)_2(Me_2phen)_2]$	dinuclear	SMM, 31.6 (0 Oe)	4
$[Zn(\mu\text{-}L')(\mu\text{-}L^4)Dy(NO_3)_2]\cdot 2CH_3CN$[b]	dinuclear	SMM, 32.1 (1 kOe)	5
$[Zn(\mu\text{-}L')(\mu\text{-}L^4)Er(NO_3)_2]\cdot 2CH_3CN$	dinuclear	n.a.	5
$[Zn(\mu\text{-}L')(\mu\text{-}L^4)Yb(NO_3)_2]\cdot 2CH_3CN$	dinuclear	n.a.	5
$[Zn(\mu\text{-}L')(\mu\text{-}L^4)Yb(L^4)(NO_3)_3]\cdot 3CH_3CN$	dinuclear	n.a.	5
$[Ni(\mu\text{-}L')(\mu\text{-}L^4)Dy(L^4)(NO_3)_2]\cdot 3CH_3CN$	dinuclear	SMM, 10.1 (1 kOe)	6
$Dy(L^3)(NO_3)_3(hmpa)_2$[c]	mononuclear	field-SMM, 20.4 (500 Oe)	7
$Dy(L^3)_3(NO_3)_3$	mononuclear	field-SMM, 35.2K (1 kOe)	8
$Dy(L^3)_4(NO_3)_2(CF_3SO_3)$	mononuclear	SMM, 26.0 (500 Oe)	8
$\{[Dy(L^2)((NH_2)_2\text{-}bdc)_{0.5}(DMF)_2]\cdot DMF\cdot H_2O\}_n$[d]	3D MOF	no SMM	9
$[Cp_2ErL^5]_2$	dinuclear	n.a.	10
$\{Dy(L^4)_3\}_n$	chain	n.a.	11
$\{Er(L^4)_3\}_n$	chain	n.a.	11
$\{Yb(L^4)_3\}_n$	chain	n.a.	11
$[Er_2(L^4)_6(1,10\text{-phenanthroline})_2]$	dinuclear	n.a.	12
$[Er_2(L^4)_6(DMF)_2(H_2O)_2]$	dinuclear	n.a.	13
$[Dy(L^6)_{1.5}(H_2O)_2(DMF)]\cdot 2DMF$	3D MOF	n.a.	14
$[Er(hfac)_3(PB\text{-}L^7)]$[e]	mononuclear	n.a.	15
$[Yb(hfac)_3(PB\text{-}L^7)]$	mononuclear	n.a.	15
$[Dy(L^3)_2(H_2O)_6]Cl_3\cdot xH_2O\cdot yCH_3OH$	mononuclear	SMM, 40.5 (1 kOe)	This work
$[Gd(L^3)_2(H_2O)_6]Cl_3\cdot xH_2O\cdot yCH_3OH$	mononuclear	field-SMM, 9.8 (1 kOe)	This work
$[Er(L^3)_2(H_2O)_6]Cl_3\cdot xH_2O\cdot yCH_3OH$	mononuclear	field-SMM, 20.3 (750 Oe)	This work

L^1 = 1,7-di-9-anthracene-1,6-heptadiene-3,5-dione; L^2 = 9,10-anthracenedicarboxylic acid; L^3 = 9-

diethylphosphonomethyl anthracene; L^4 = 9-anthracenecarboxylate; L^5 = 1,8-diethynylanthracene; L^6 = 9,10-diethynylphenyl anthracene; L^7 = anthacenyl group.

a: hfac = hexafluoroacetylacetonated, b: H_2L'= N,N',N''-trimethyl-N,N''-bis(2-hydroxy-3-methoxy-5-methylbenzyl)diethylenetriamine, c: hmpa = hexamethylphosphoramide, d: $(NH_2)_2$-bdc = 2,5-diaminoterephthalic acid, e: PB = 2-(2-pyridyl)benzimidazole; f: n.a. = not available.

References:

[1] M. Menelaou, F. Ouharrou, L. Rodríguez, O. Roubeau, S. J. Teat and N. Aliaga-Alcade, *Chem.–Eur. J.*, 2012, **18**, 11545.

[2] A. J. Calahorro, I. Oyarzabal, B. Fernández, J. M. Seco, T. Tian, D. Fairen-Jimenez and E. Colacio, *Dalton Trans.*, 2016, **45**, 591.

[3] D.-K. Cao, Y.-W. Gu, J.-Q. Feng, Z.-S. Cai and M. D. Ward, *Dalton Trans.*, 2013, **42**, 11436.

[4] Y.-L. Wang, C.-B. Han, Y.-Q. Zhang, Q.-Y. Liu, C.-M. Liu and S.-G. Yin, *Inorg. Chem.,* 2016, **55**, 5578.

[5] M. A. Palacios, S. Titos-Padilla, J. Ruiz, J. M. Herrera, S. J. A. Pope, E. K. Brechin and E. Colacio, *Inorg. Chem.*, 2014, **53**, 1465.

[6] E. Colacio, J. Ruiz, A. J. Mota, M. A. Palacios, E. Cremades, E. Ruiz, F. J. White, and E. K. Brechin, *Inorg. Chem.*, 2012, **51**, 5857.

[7] X.-D. Huang, Y. Xu, K. Fan, S.-S. Bao, M. Kurmoo, and L.-M. Zheng, *Angew. Chem. Int. Ed.*, 2018, **57**, 8577.

[8] X.-D. Huang, M. Kurmoo, S.-S. Bao, K. Fan, Y. Xu, Z.-B. Hu and L.-M. Zheng, *Chem. Commun.*, 2018, **54**, 3278.

[9] I. Oyarzabal, B. Fernández, J. peda, S.Gómez-Ruiz, A.J. Calahorro, J. M. Seco and A. Rodríguez-Diéguez, *CrystEngComm,* 2016, **18**, 3055.

[10] M. Pieper, J.-H. Lamm, B. Neumann, H.-G. Stammler and N. W. Mitzel, *Dalton Trans.*, 2017, **46**, 5326.

[11] V. V. Utochnikova, A. S. Kalyakina, I. S. Bushmarinov, A. A. Vashchenko, L. Marciniak, A. M. Kaczmarek, R. V. Deun, S. Bräse and N. P. Kuzmina, *J. Mater. Chem. C*, 2016, **4**, 9848.

[12] C.-S. Liu, L.-Q. Guo, L.-F. Yan and J.-J. Wang, Acta Crystallogr., *Sect. C: Cryst. Struct. Commun.,* 2008, **C64**, m292.

[13] E. Kusrini, R. Adnan, M. I. Saleh, L.-K. Yan and H.-K. Fun, *Spectrochim. Acta, Part A*, 2009, **72**, 884.

[14] Q.-S. Xia, X.-D. Yu, H.-M. Zhao, S.-P. Wang, H. Wang, Z.-F Guo, and H.-Z Xing, *Cryst. Growth Des.*, 2017, **17**, 4189.

[15] T. Lazarides, M. A. H. Alamiry, H. Adams, S. J. A. Pope, S. Faulkner, J. A. Weinstein and M. D. Ward, *Dalton Trans.*, 2007, 1484.

Table S2. Selected bond lengths (Å) and bond angles (°) for **1Dy** at 123 K.

Dy1-O1	2.279(9)	O1W-Dy1-O1A	84.2(3)
Dy1-O1W	2.371(8)	O1W-Dy1-O1WA	149.9(3)
Dy1-O2W	2.429(12)	O2W-Dy1-O3W	130.7(5)
Dy1-O3W	2.445(12)	O2W-Dy1-O4W	143.6(5)
Dy1-O4W	2.333(14)	O2W-Dy1-O5W	132.2(6)
Dy1-O5W	2.387(12)	O2W-Dy1-O1A	80.0(5)
O1-Dy1-O1W	86.2(3)	O2W-Dy1-O1WA	75.3(5)
O1-Dy1-O2W	62.4(5)	O3W-Dy1-O4W	78.4(5)
O1-Dy1-O3W	83.9(4)	O3W-Dy1-O5W	69.4(4)
O1-Dy1-O4W	153.3(4)	O3W-Dy1-O1A	124.8(4)
O1-Dy1-O5W	81.8(4)	O3W-Dy1-O1WA	139.0(3)
O1-Dy1-O1A	142.4(4)	O4W-Dy1-O5W	73.4(4)
O1-Dy1-O1WA	84.2(3)	O4W-Dy1-O1A	63.9(4)
O1W-Dy1-O2W	74.9(5)	O4W-Dy1-O1WA	96.3(4)
O1W-Dy1-O3W	67.6(3)	O5W-Dy1-O1A	128.2(4)
O1W-Dy1-O4W	104.8(4)	O5W-Dy1-O1WA	70.2(4)
O1W-Dy1-O5W	136.3(4)		

Symmetry transformations used to generate equivalent atoms: A: 1-x, y, 0.5-z.

Table S3. Continuous Shape Measure (CShM) analyses of dysprosium geometries for **1Dy**-**3Er** using the SHAPE2.1 Software.

Geometry	**1Dy**	**2Gd**	**3Er**
Octagon (D_{8h})	33.845	33.869	34.172
Heptagonal pyramid (C_{7v})	22.626	22.512	22.477
Hexagonal bipyramid (D_{6h})	16.860	16.640	16.692
Cube (O_h)	12.150	12.125	12.080
Square antiprism (D_{4d})	3.712	3.761	3.853
Triangular dodecahedron (D_{2d})	1.485	1.447	1.451
Johnson gyrobifastigium J26 (D_{2d})	12.815	12.822	12.702
Johnson elongated triangular bipyramid J14 (D_{3h})	26.883	26.854	26.926
Biaugmented trigonal prism J50 (C_{2v})	2.635	2.681	2.765
Biaugmented trigonal prism (C_{2v})	2.070	2.075	2.198
Snub diphenoid J84 (D_{2d})	3.366	3.410	3.354
Triakis tetrahedron (T_d)	12.534	12.559	12.453
Elongated trigonal bipyramid (D_{3h})	23.095	23.041	23.142

Table S4. The parameters of and H-bonding for **1Dy**.

D-H⋯A	$d_{D\cdots A}$(Å)	$D_{H\cdots A}$(Å)	$Angle_{D\text{-}H\cdots A}$(°)
O1W[a]-H1WA⋯Cl2[b]	3.274	2.530	146.00
O1W[a]-H1WB⋯Cl1[b]	3.142	2.570	126.00
O2W[a]-H2WB⋯O6W[a]	2.370	2.000	105.00
O3W[a]-H3WA⋯Cl1[c]	3.131	2.580	123.00
O3W[a]-H3WB⋯Cl1[b]	2.901	2.080	163.00
O4W[a]-H4WA⋯Cl1[d]	3.098	2.430	136.00
O4W[a]-H4WB⋯Cl1[e]	3.346	2.540	156.00
O5W[a]-H5WA⋯Cl1[a]	2.945	2.330	130.00
O5W[a]-H5WB⋯O5W[d]	3.003	2.370	132.00
O6W[a]-H6WB⋯Cl2[a]	2.405	1.960	112.00
O1W[e]-H1WB⋯Cl1[a]	2.947	2.130	160.00
C11[a]-H11⋯π[f]	3.291	2.730	118.00

Symmetry transformations used to generate equivalent atoms: (a) x, y, z; (b) x, y, -1+z; (c) x, -y, -0.5+z; (d) 1-x, -y, 1-z; (e) 1-x, y, 0.5-z; (f) 0.5+x, 0.5+y, 0.5-z.

Table S5. Selected bond lengths (Å) and bond angles (°) for **2Gd** at 150 K.

Gd1-O1	2.317(10)	O1W-Gd1-O1A	84.0(3)
Gd1-O1W	2.403(10)	O1W-Gd1-O1WA	150.6(3)
Gd1-O2W	2.454(16)	O2W-Gd1-O3W	129.6(6)
Gd1-O3W	2.452(17)	O2W-Gd1-O4W	144.3(6)
Gd1-O4W	2.375(17)	O2W-Gd1-O5W	132.6(8)
Gd1-O5W	2.410(15)	O2W-Gd1-O1A	79.9(5)
O1-Gd1-O1W	86.7(3)	O2W-Gd1-O1WA	76.1(7)
O1-Gd1-O2W	62.6(5)	O3W-Gd1-O4W	78.6(6)
O1-Gd1-O3W	83.2(5)	O3W-Gd1-O5W	69.4(5)
O1-Gd1-O4W	152.4(5)	O3W-Gd1-O1A	125.1(5)
O1-Gd1-O5W	81.3(5)	O3W-Gd1-O1WA	138.9(4)
O1-Gd1-O1A	142.5(4)	O4W-Gd1-O5W	73.0(5)
O1-Gd1-O1WA	84.0(3)	O4W-Gd1-O1A	64.7(5)
O1W-Gd1-O2W	74.9(7)	O4W-Gd1-O1WA	96.3(4)
O1W-Gd1-O3W	66.8(4)	O5W-Gd1-O1A	128.8(5)
O1W-Gd1-O4W	104.6(4)	O5W-Gd1-O1WA	70.1(4)
O1W-Gd1-O5W	135.6(4)		

Symmetry transformations used to generate equivalent atoms: A: 1-x, y, 0.5-z.

Table S6. Selected bond lengths (Å) and bond angles (°) for **3Er** at 150 K.

Er1-O1	2.266(6)	O1W-Er1-O1A	83.8(2)
Er1-O1W	2.345(6)	O1W-Er1-O1WA	150.3(2)
Er1-O2W	2.406(8)	O2W-Er1-O3W	129.5(4)
Er1-O3W	2.413(11)	O2W-Er1-O4W	144.0(4)
Er1-O4W	2.308(11)	O2W-Er1-O5W	132.2(4)
Er1-O5W	2.360(9)	O2W-Er1-O1A	80.0(3)
O1-Er1-O1W	86.6(2)	O2W-Er1-O1WA	75.6(4)
O1-Er1-O2W	62.1(3)	O3W-Er1-O4W	78.7(4)
O1-Er1-O3W	83.3(3)	O3W-Er1-O5W	70.0(3)
O1-Er1-O4W	153.4(3)	O3W-Er1-O1A	125.2(3)
O1-Er1-O5W	82.0(3)	O3W-Er1-O1WA	139.2(3)
O1-Er1-O1A	142.1(3)	O4W-Er1-O5W	73.6(4)
O1-Er1-O1WA	83.8(2)	O4W-Er1-O1A	64.3(3)
O1W-Er1-O2W	75.1(4)	O4W-Er1-O1WA	97.2(3)
O1W-Er1-O3W	66.7(3)	O5W-Er1-O1A	128.3(3)
O1W-Er1-O4W	103.7(3)	O5W-Er1-O1WA	69.9(3)
O1W-Er1-O5W	136.2(3)		

Symmetry transformations used to generate equivalent atoms: A: 1-x, y, 0.5-z.

Table S7. The fit parameters obtained from analyses of the ac susceptibilities of **1Dy** under 1 kOe bias dc field in the frequency range of 1-1488 Hz.

T / K	χ_T / cm^3 mol^{-1}	χ_S / cm^3 mol^{-1}	ln(τ / s)	α	Residual
1.8	6.60967	0.71329	-2.85968	0.40696	5.337×10^{-2}
2.0	5.81068	0.64774	-3.2871	0.38564	3.868×10^{-2}
2.2	5.28566	0.60533	-3.61048	0.36602	3.803×10^{-2}
2.4	4.75066	0.56588	-4.00089	0.34064	4.239×10^{-2}
2.6	4.37428	0.53519	-4.3377	0.31869	4.873×10^{-2}
2.8	4.0486	0.51181	-4.69465	0.29596	4.633×10^{-2}
3.0	3.76906	0.49627	-5.06339	0.2723	4.323×10^{-2}
3.3	3.4355	0.47125	-5.64593	0.24846	3.244×10^{-2}
3.6	3.16683	0.44247	-6.24945	0.2375	2.247×10^{-2}
3.9	2.94231	0.43695	-6.8536	0.23256	1.474×10^{-2}
4.2	2.7511	0.43872	-7.44675	0.23293	1.11×10^{-2}
4.5	2.59393	0.44906	-8.02309	0.24902	1.042×10^{-2}
4.8	2.44161	0.51067	-8.53106	0.2454	6.41×10^{-3}
5.1	2.30828	0.60108	-8.97282	0.23601	4.11×10^{-3}

Table S8. The fit parameters obtained from analyses of the ac susceptibilities of **4Yb** under 750 Oe bias dc field in the frequency range of 11-1488 Hz.

T / K	χ_T / cm^3 mol^{-1}	χ_S / cm^3 mol^{-1}	ln(τ / s)	α	Residual
1.8	0.719063	0.11564	-7.43776	0.13792	9.12789×10^{-4}
2.0	0.658529	0.10187	-7.68429	0.13247	6.48348×10^{-4}
2.2	0.614117	0.09935	-7.85095	0.12232	4.82357×10^{-4}
2.4	0.563115	0.0865	-8.10928	0.11906	5.35517×10^{-4}
2.6	0.525134	0.0769	-8.3211	0.12656	4.42807×10^{-4}
2.8	0.489837	0.06893	-8.53681	0.12799	4.55034×10^{-4}
3.0	0.459927	0.05722	-8.7805	0.13984	4.25602×10^{-4}
3.2	0.433313	0.04262	-9.0284	0.15324	3.65557×10^{-4}
3.4	0.409220	0.02637	-9.2917	0.16551	3.69117×10^{-4}
3.6	0.387798	1.20968×10^{-7}	-9.63811	0.19085	4.64218×10^{-4}
3.8	0.367601	1.55617×10^{-7}	-9.85939	0.19063	3.5289×10^{-4}
4.0	0.350559	2.38505×10^{-7}	-10.1348	0.21233	4.32627×10^{-4}

Table S9. The emission lifetimes at room temperature for the solid compound **1Dy–4Yb** excited at 374nm.

compound	λ_{em}/ nm	τ_1/ ns	τ_2/ ns	τ_3/ ns	$\tau_{average}$/ ns	χ^2
1Dy	430	1.29 (46.74 %)	4.30 (53.26 %)	-	2.06	1.07
2Gd	430	0.41 (13.03 %)	1.44 (67.82 %)	4.35 (19.15 %)	1.20	1.24
3Er	430	0.37 (20.85 %)	0.99 (73.61 %)	4.82 (5.54 %)	0.76	1.13
4Yb	430	0.76 (24.66 %)	5.77 (75.34 %)	-	2.19	1.11

(a)

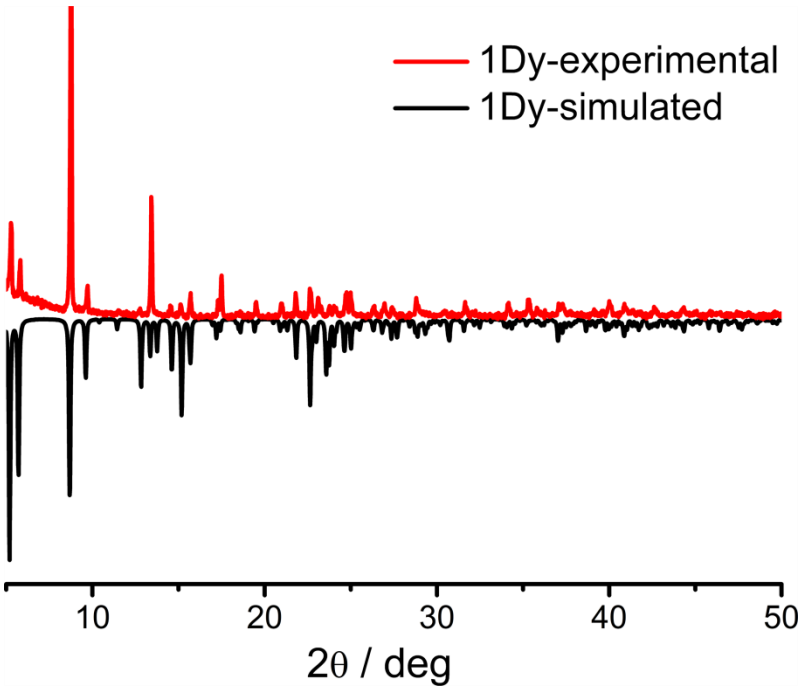
1Dy-experimental
1Dy-simulated
10
20
30
40
50
2θ / deg

(b)

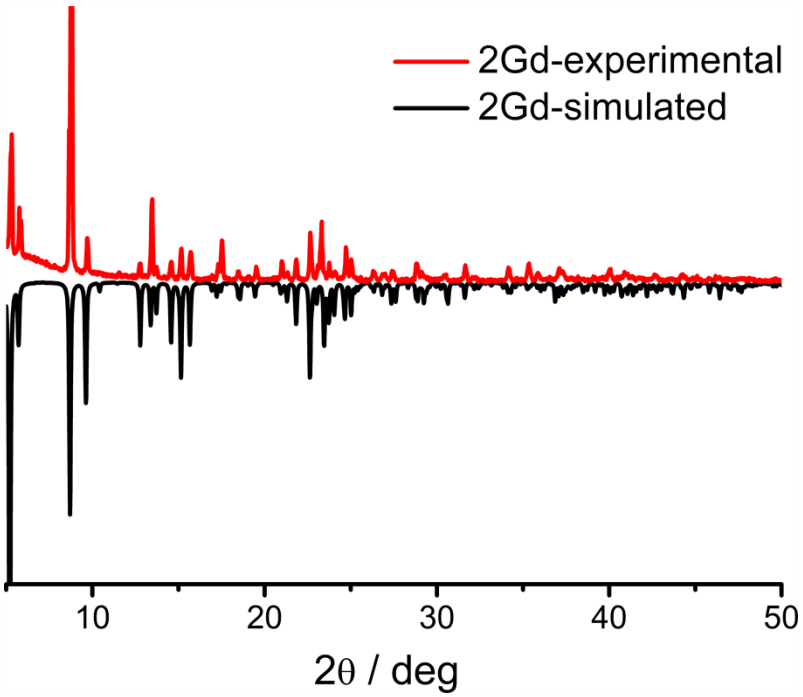
2Gd-experimental
2Gd-simulated
10
20
30
40
50
2θ / deg

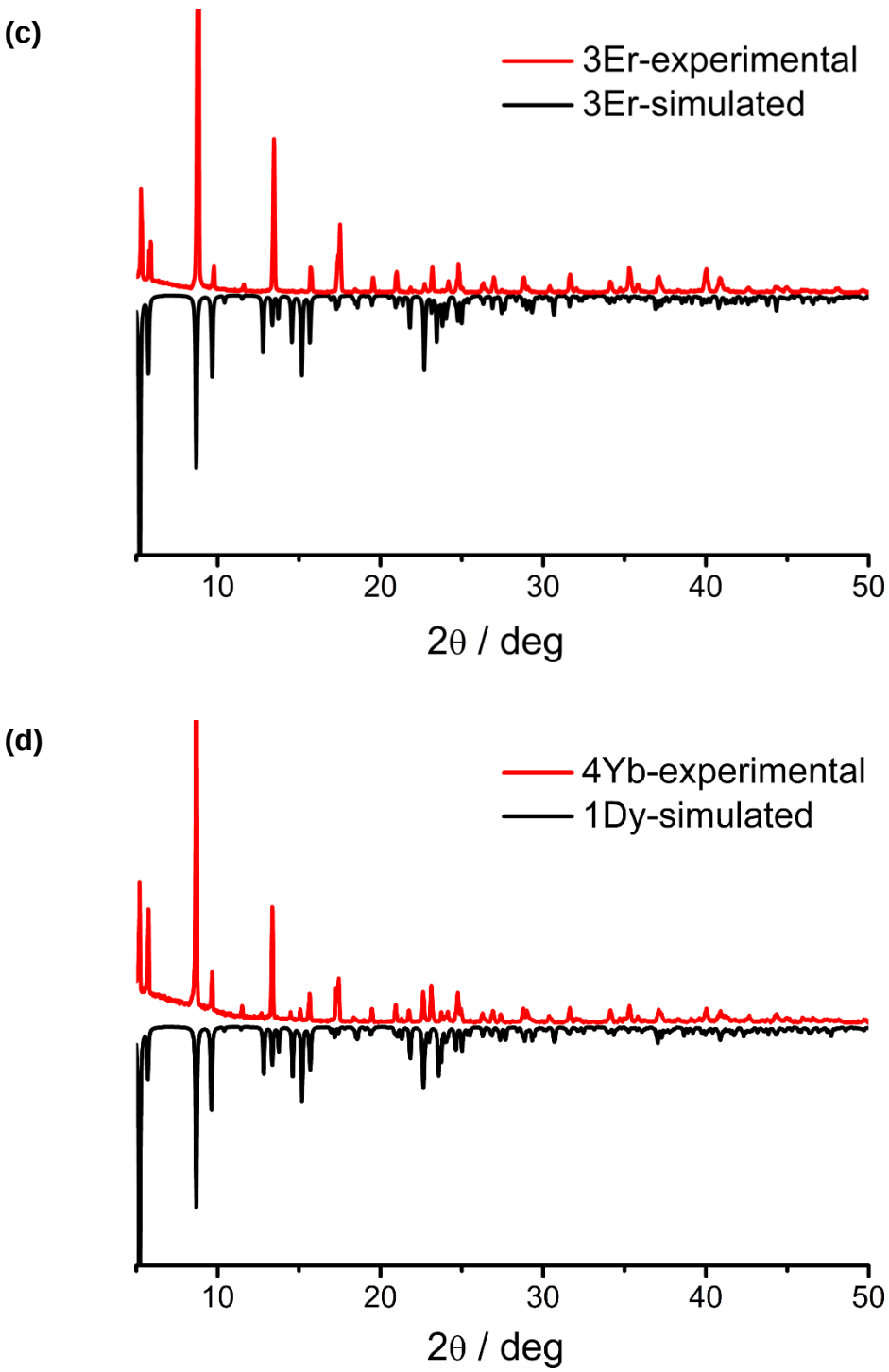

Figure S1. Experimental (red) and simulated (black) PXRD patterns for compounds **1Dy** (a), **2Gd** (b), **3Er** (c) and **4Yb** (d). The simulated PXRD pattern of **1Dy** was given in (d) for a comparison.

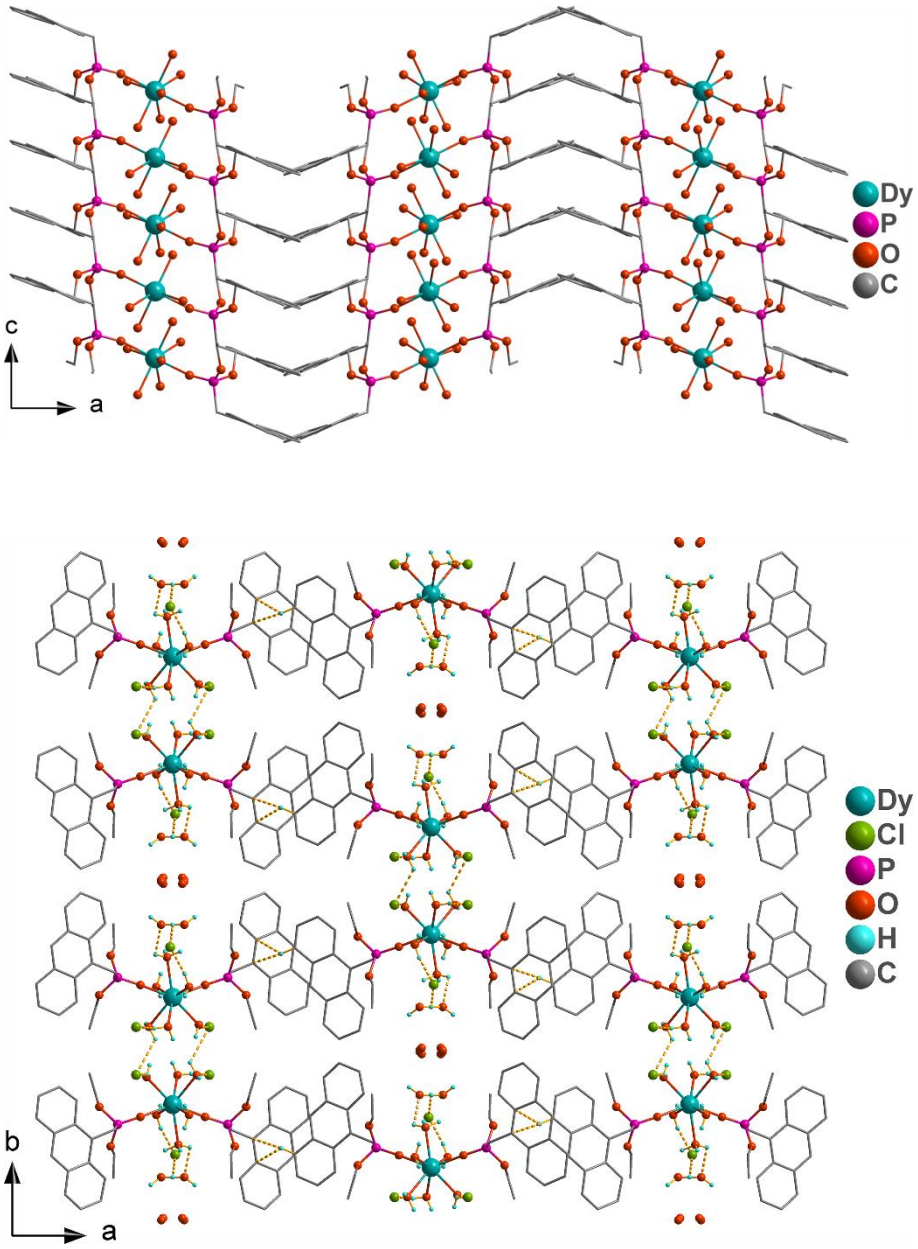

Figure S2. Top: The packing diagrams of **1Dy** with the view along the b-axis. Bottom: The H-bonds interactions between compound **1Dy** with the view along the c axis.

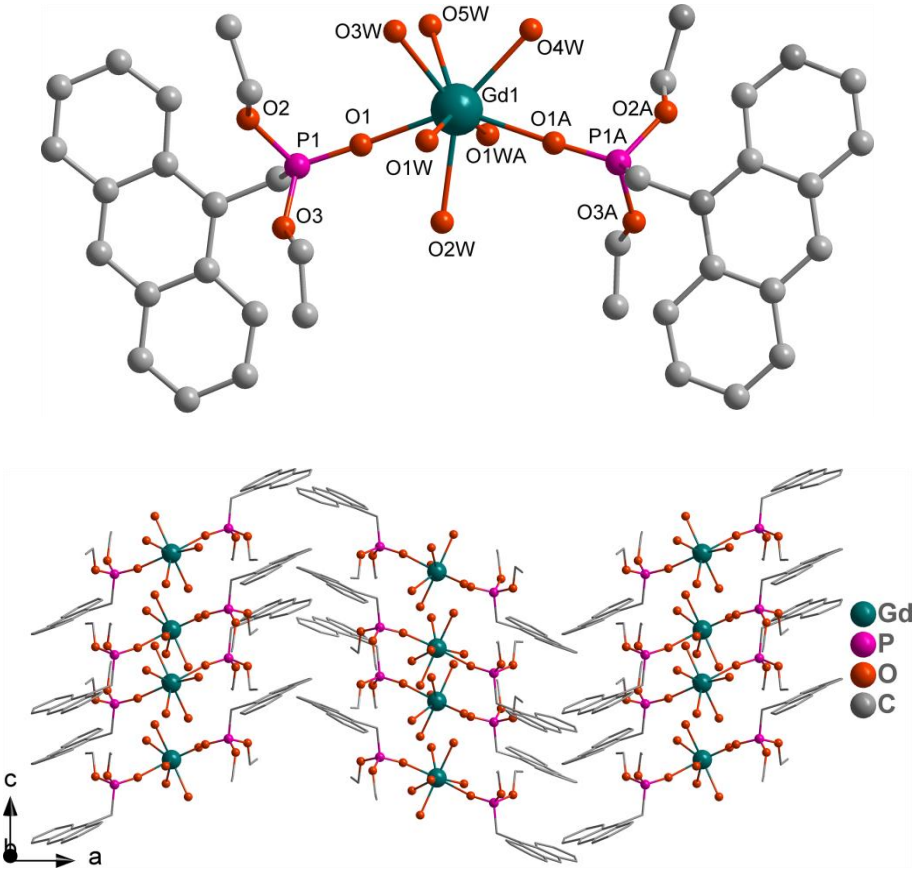

Figure S3. Top: The fragment of the crystal structure of **2Gd.** Bottom: The packing diagram of **2Gd** with the view approximately along the b-axis. For clarity, All hydrogen atoms are omitted.

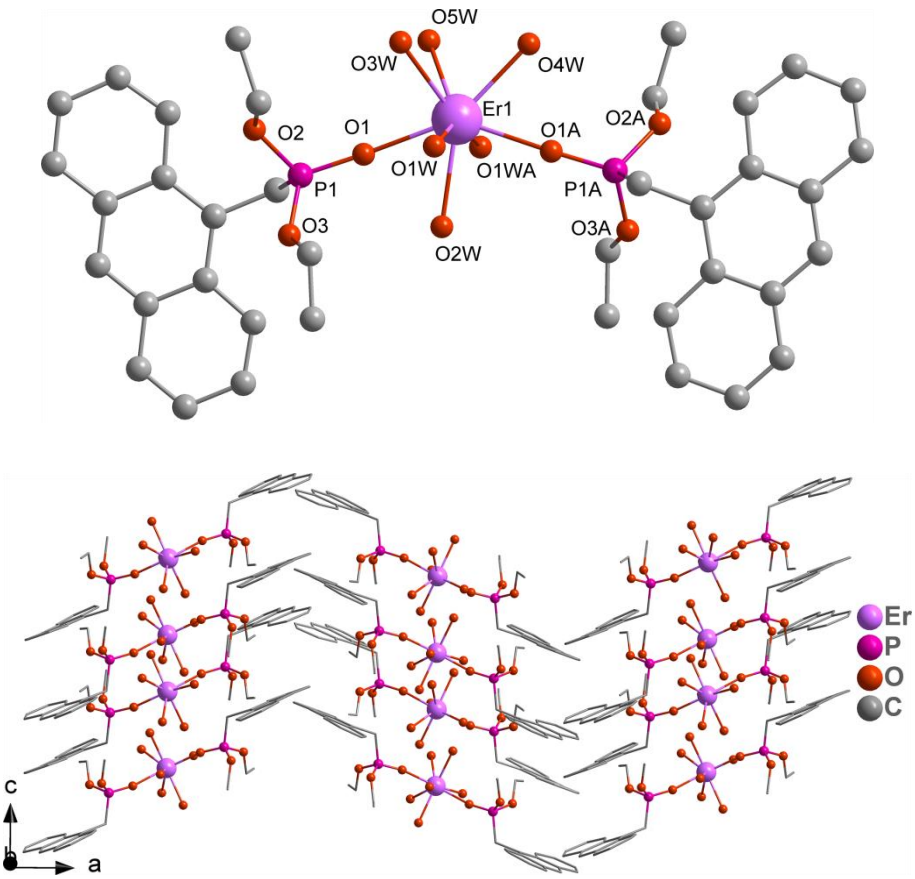

Figure S4. Top: The fragment of the crystal structure of **3Er.** Bottom: The packing diagram of **3Er** with the view approximately along the b-axis. For clarity, All hydrogen atoms are omitted.

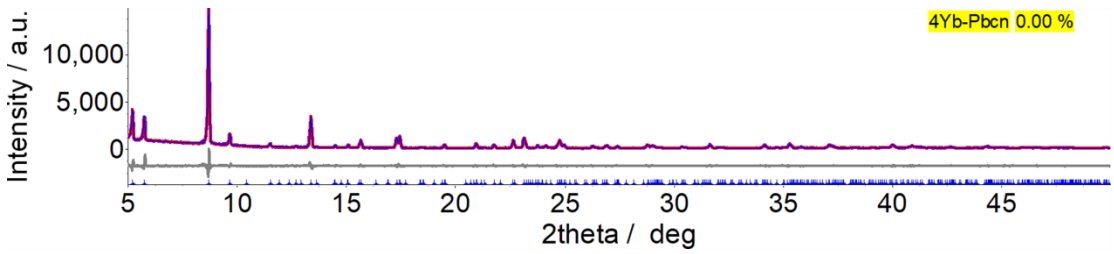

Figure S5. Pawley fit of a powder sample of compound **4Yb** performed using *Topas* 5.0 program. Blue is the measured intensities, red is the calculated intensities, and gray is the difference plot between the measured and calculated intensities (Rwp : 9.7, GOF : 2.0).

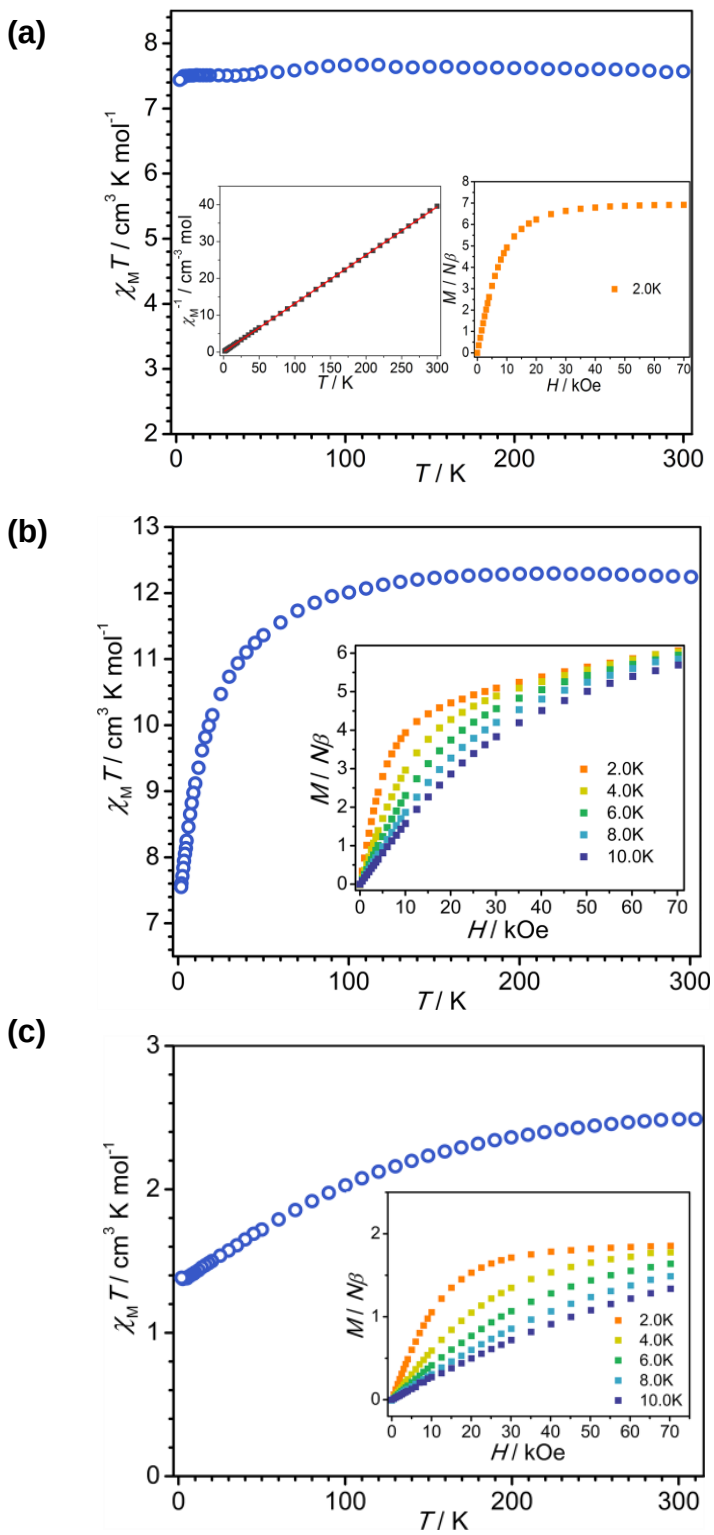

Figure S6. Temperature dependence of $\chi_M T$ on cooling in a field of 1 kOe for **2Gd** (a), **3Er** (b) and **4Yb** (c). Inset: Field dependence of the magnetization at 2K for **2Gd** (a) and at depicted temperatures for compound **3Er** (b) and **4Yb** (c). The χ_M^{-1} vs. *T* curve for **2Gd** is also presented (a, inset).

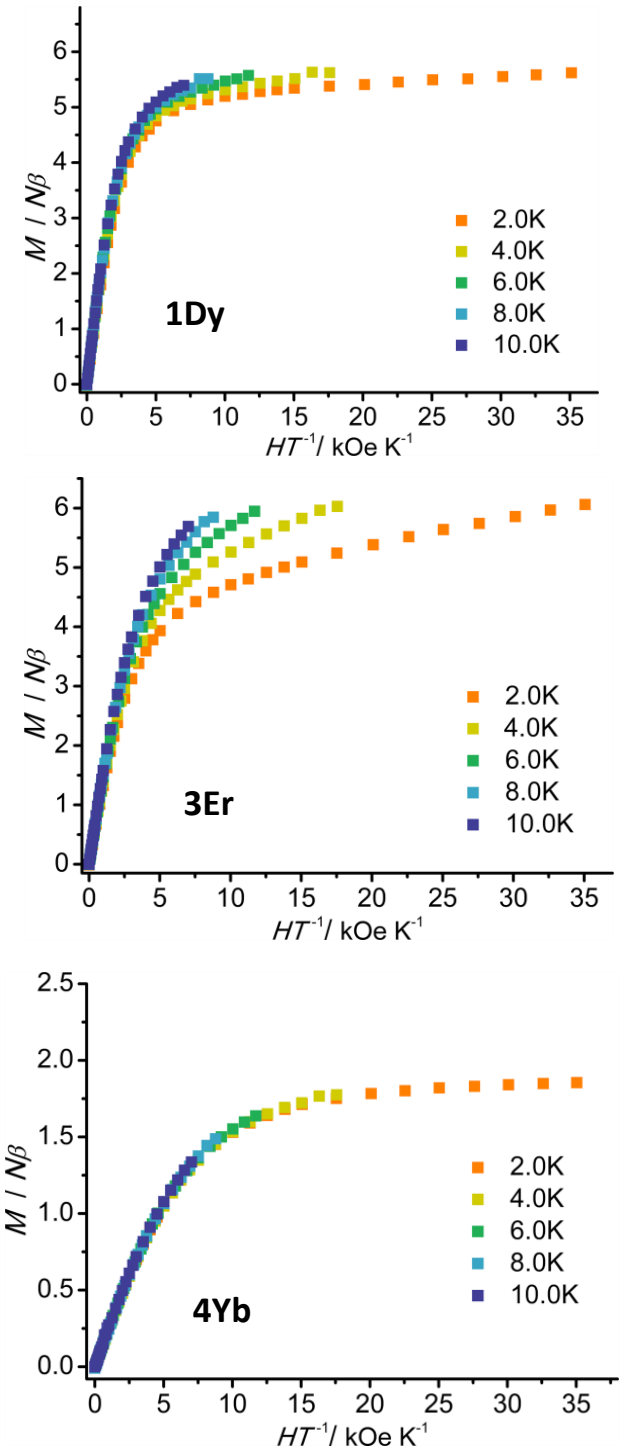

Figure S7. The plots of magnetization *M* versus *H*/*T* at depicited temperatures for compounds **1Dy**, **3Er** and **4Yb**.

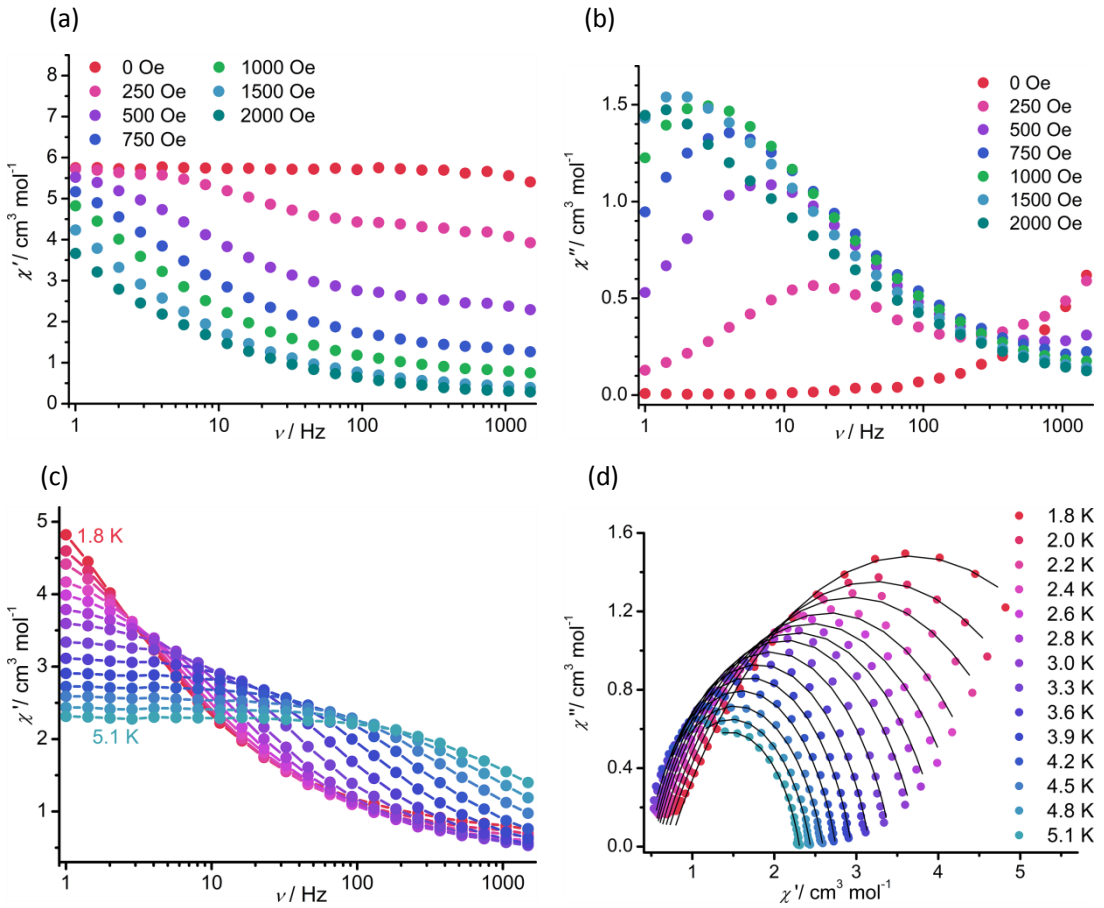

Figure S8. Frequency dependence of the in-phase (a) and out-of-phase (b) signals for **1Dy** in the indicated dc fields at 1.8 K. (c) Frequency dependence of the in-phase (χ') ac susceptibilities and (d) Cole-Cole plots for **1Dy**, measured in the temperature range 1.8-5.0 K under 1000 Oe dc field. The solid line represents the best fit using a generalized Debye model.

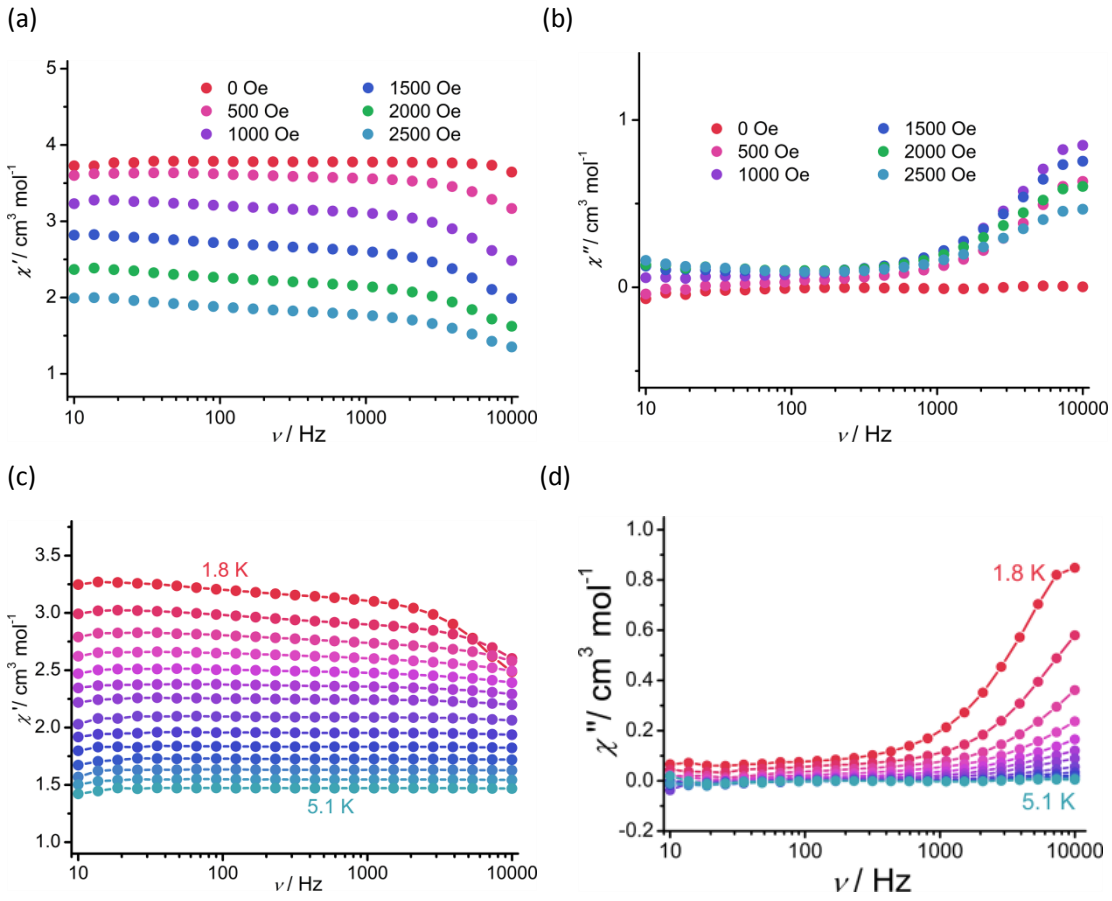

Figure S9. Frequency dependence of the in-phase (a) and out-of-phase (b) signals for **3Er** in the indicated dc fields at 1.8 K. (c) Frequency dependence of the in-phase (χ') and out-of-phase (χ'') ac susceptibilities signals for **3Er**, measured in the temperature range 1.8-5.1 K under 1000 Oe dc field.

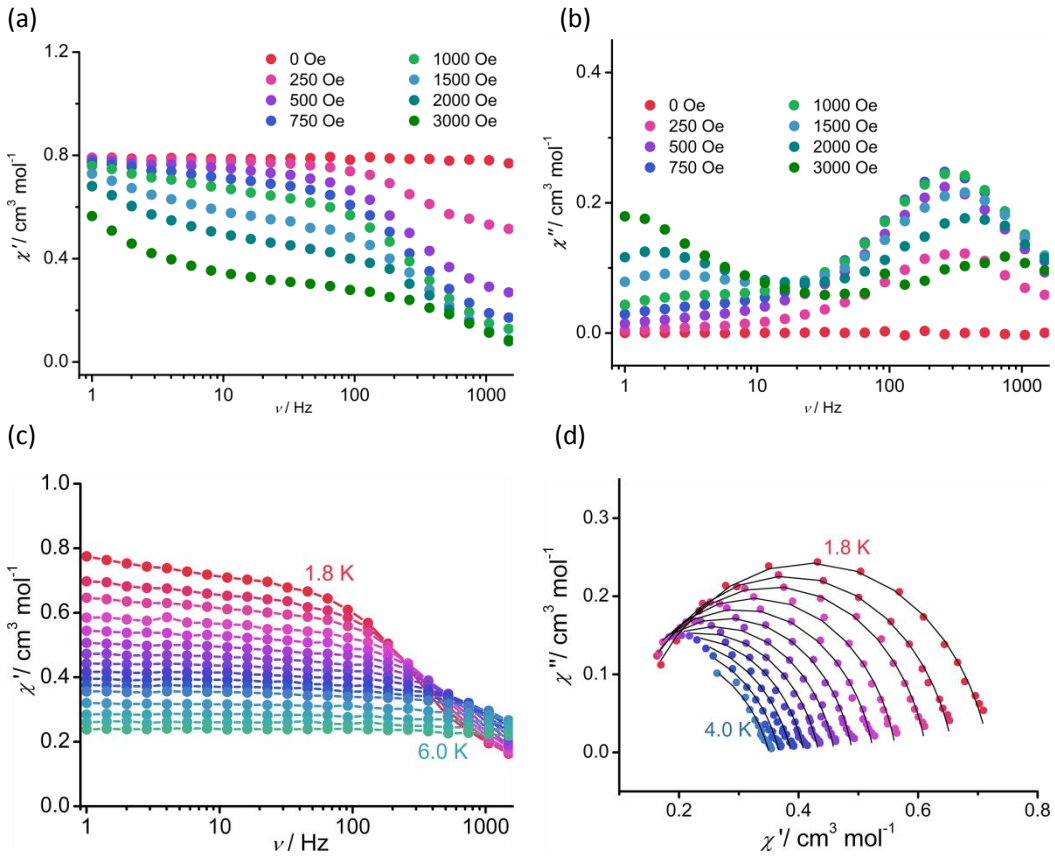

Figure S10. Frequency dependence of the in-phase (a) and out-of-phase (b) signals for **4Yb** in the indicated dc fields at 1.8 K. (c) Frequency dependence of the in-phase (χ') ac susceptibilities in the frequency range of 1-1488 Hz for **4Yb**, measured in the temperature range 1.8-6.0 K under 750 Oe dc field. (d) Cole-Cole plots for **4Yb**, measured in the temperature range 1.8-4.0 K under 750 Oe dc field in the frequency range of 11-1488 Hz for **4Yb**. The solid line represents the best fitting.

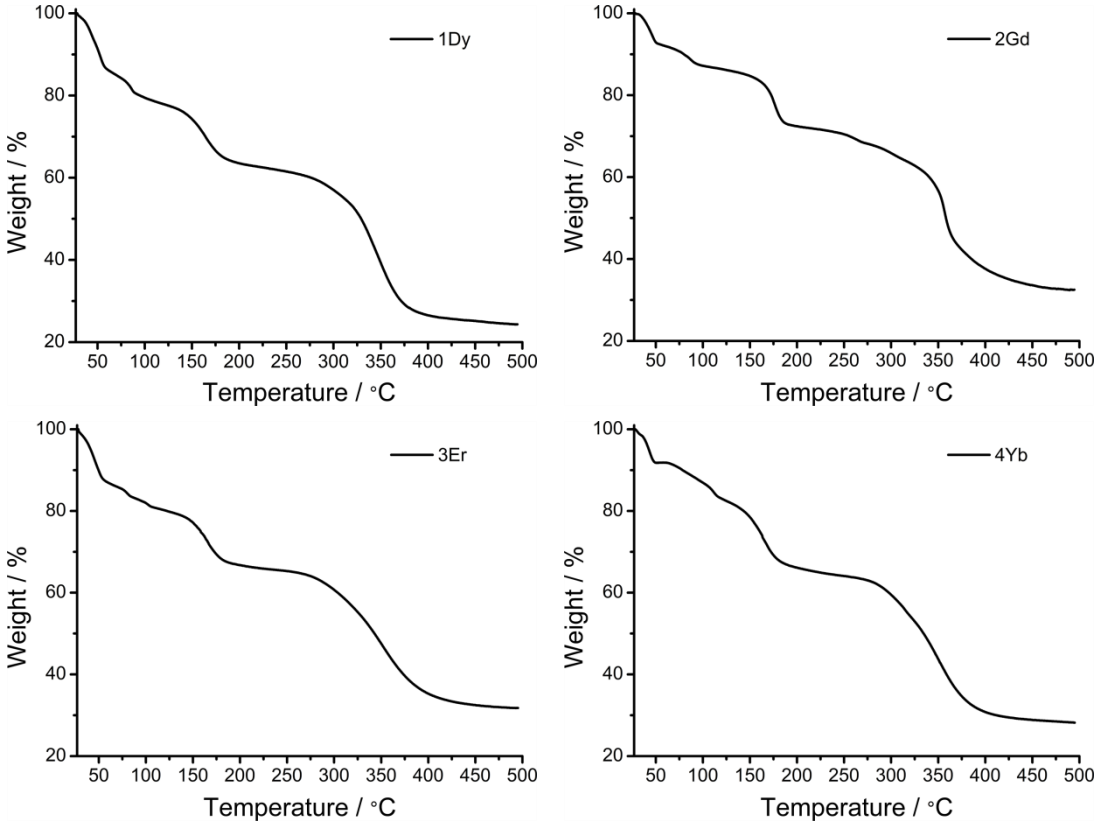

Figure S11. Thermogravimetric curves of Compounds **1Dy – 4Yb** measured over a temperature range of 25-500 °C. The molecular formula of the compounds obtained from the weight loss curve are in good agreement with the results of the elemental analysis.